

August, 1995

QCD corrections to the decay $H^+ \rightarrow t\bar{b}$ in the Minimal Supersymmetric Standard Model

A. Bartl,¹ H. Eberl,² K. Hidaka,³ T. Kon,⁴
 W. Majerotto² and Y. Yamada⁵

¹*Institut für Theoretische Physik, Universität Wien, A-1090 Vienna, Austria*

²*Institut für Hochenergiephysik der Österreichische Akademie der Wissenschaften, A-1050 Vienna, Austria*

³*Department of Physics, Tokyo Gakugei University, Koganei, Tokyo 184, Japan*

⁴*Faculty of Engineering, Seikei University, Musashino, Tokyo 180, Japan*

⁵*Theory Group, National Laboratory for High Energy Physics (KEK), Tsukuba, Ibaraki 305, Japan*

Abstract

We calculate the supersymmetric $\mathcal{O}(\alpha_s)$ QCD corrections to the width of the decay $H^+ \rightarrow t\bar{b}$ within the Minimal Supersymmetric Standard Model. We find that the QCD corrections are significant, but that they do not invalidate our previous conclusion at tree-level on the dominance of the $t\bar{b}$ mode in a wide parameter region.

1 Introduction

In the Minimal Supersymmetric Standard Model (MSSM) [1, 2] two Higgs doublets are necessary, leading to five physical Higgs bosons h^0, H^0, A^0 , and H^\pm [3, 4]. If all supersymmetric (SUSY) particles are very heavy, the charged Higgs boson H^+ decays dominantly into $t\bar{b}$; the decays $H^+ \rightarrow \tau^+\nu$ and/or $H^+ \rightarrow W^+h^0$ are dominant below the $t\bar{b}$ threshold [3, 5]. In ref. [6] all decay modes of H^+ including the SUSY-particle modes were studied in detail; it was shown that the SUSY decay modes $H^+ \rightarrow \tilde{t}_i \tilde{\bar{b}}_j (i, j = 1, 2)$ can be dominant in a large region of the MSSM parameter space due to large t and b quark Yukawa couplings and large \tilde{t} - and \tilde{b} -mixings, and that this could have a decisive impact on H^+ searches at future colliders. Here \tilde{t}_i (\tilde{b}_j) are the scalar top (scalar bottom) mass eigenstates which are mixtures of \tilde{t}_L and \tilde{t}_R (\tilde{b}_L and \tilde{b}_R).

The standard QCD corrections are very large for the width of $H^+ \rightarrow c\bar{s}$ and can be large (+10% to -50%) for that of $H^+ \rightarrow t\bar{b}$ [7]. The QCD corrections from the SUSY-particle loops are calculated within the MSSM for $H^+ \rightarrow t\bar{b}$ in [8] and turn out to be non-negligible ($\sim 10\%$) for certain values of the MSSM parameters. This suggests that the QCD corrections to $H^+ \rightarrow \tilde{t} \tilde{\bar{b}}$ could also be large. Therefore it should be examined whether the result in [6] remains valid after including the QCD corrections.

In this paper we calculate the $\mathcal{O}(\alpha_s)$ QCD corrections to the width of $H^+ \rightarrow \tilde{t}_i \tilde{\bar{b}}_j$ within the MSSM. To the best of our knowledge they are not known in the literature. We obtain the complete $\mathcal{O}(\alpha_s)$ corrected width in the $\overline{\text{DR}}$ renormalization

scheme (i.e. the $\overline{\text{MS}}$ scheme with dimensional reduction [9]) including all quark mass terms and $\tilde{q}_L - \tilde{q}_R$ mixings. The main complication here is that the $\tilde{q}_L - \tilde{q}_R$ mixing angles are renormalized by the SUSY QCD corrections. We find that the corrections to the $\tilde{t}\tilde{b}$ width are significant but that the $\tilde{t}\tilde{b}$ mode is still dominant in a wide parameter range.

2 Tree level result

We first review the tree level results [6]. The squark mass matrix in the basis $(\tilde{q}_L, \tilde{q}_R)$, with $\tilde{q} = \tilde{t}$ or \tilde{b} , is given by [3, 4]

$$\begin{pmatrix} m_{LL}^2 & m_{LR}^2 \\ m_{RL}^2 & m_{RR}^2 \end{pmatrix} = (R^{\tilde{q}})^\dagger \begin{pmatrix} m_{\tilde{q}_1}^2 & 0 \\ 0 & m_{\tilde{q}_2}^2 \end{pmatrix} R^{\tilde{q}}, \quad (1)$$

where

$$m_{LL}^2 = M_{\tilde{Q}}^2 + m_q^2 + m_Z^2 \cos 2\beta (I_q - Q_q \sin^2 \theta_W), \quad (2)$$

$$m_{RR}^2 = M_{\{\tilde{U}, \tilde{D}\}}^2 + m_q^2 + m_Z^2 \cos 2\beta Q_q \sin^2 \theta_W, \quad (3)$$

$$m_{LR}^2 = m_{RL}^2 = \begin{cases} m_t(A_t - \mu \cot \beta) & (\tilde{q} = \tilde{t}) \\ m_b(A_b - \mu \tan \beta) & (\tilde{q} = \tilde{b}) \end{cases}, \quad (4)$$

and

$$R_{i\alpha}^{\tilde{q}} = \begin{pmatrix} \cos \theta_{\tilde{q}} & \sin \theta_{\tilde{q}} \\ -\sin \theta_{\tilde{q}} & \cos \theta_{\tilde{q}} \end{pmatrix}. \quad (5)$$

Here the mass eigenstates $\tilde{q}_i (i = 1, 2)$ (with $m_{\tilde{q}_1} < m_{\tilde{q}_2}$) are related to the $\text{SU}(2)_L$ eigenstates $\tilde{q}_\alpha (\alpha = L, R)$ as $\tilde{q}_i = R_{i\alpha}^{\tilde{q}} \tilde{q}_\alpha$. Note that in the sign convention used here the parameters $A_{t,b}$ correspond to $(-A_{t,b})$ of ref.[6].

The tree-level decay width of $H^+ \rightarrow \tilde{t}_i \tilde{b}_j$ is then given by (see Fig. 1a)

$$\Gamma^{(0)}(H^+ \rightarrow \tilde{t}_i \tilde{b}_j) = \frac{N_C \kappa}{16\pi m_H^3} |G_{ij}|^2, \quad (6)$$

where m_H is the H^+ mass, $\kappa = \kappa(m_H^2, m_{t_i}^2, m_{b_j}^2)$, $\kappa(x, y, z) \equiv ((x - y - z)^2 - 4yz)^{1/2}$, $N_C = 3$, and

$$G_{ij} = \frac{g}{\sqrt{2}m_W} R^{\bar{i}} \begin{pmatrix} m_b^2 \tan \beta + m_t^2 \cot \beta - m_W^2 \sin 2\beta & m_b(A_b \tan \beta + \mu) \\ m_t(A_t \cot \beta + \mu) & 2m_t m_b / \sin 2\beta \end{pmatrix} (R^{\bar{b}})^\dagger \quad (7)$$

are the $H^+ \tilde{t}_i \tilde{b}_j$ couplings [3, 4], with g being the SU(2) coupling.

3 QCD virtual corrections

The $\mathcal{O}(\alpha_s)$ QCD virtual corrections to $H^+ \rightarrow \tilde{t}_i \tilde{b}_j$ stem from the diagrams of Fig. 1b (vertex corrections) and 1c (wave function corrections). For simplicity we use in this paper the $\overline{\text{DR}}$ renormalization scheme* for all parameters which receive the QCD corrections, i.e. $m_{t,b}$, $A_{t,b}$, and $M_{\tilde{Q}, \tilde{U}, \tilde{D}}$. The renormalized squark mixing angle $\theta_{\tilde{q}}$ is then defined by the relations (1–5) in terms of the $\overline{\text{DR}}$ parameters $m_{t,b}$, $A_{t,b}$, and $M_{\tilde{Q}, \tilde{U}, \tilde{D}}$.

The one-loop corrected decay amplitudes G_{ij}^{corr} are expressed as

$$G_{ij}^{\text{corr}} = G_{ij} + \delta G_{ij}^{(v)} + \delta G_{ij}^{(w)}, \quad (8)$$

where G_{ij} are defined by (7) in terms of the $\overline{\text{DR}}$ parameters, and $\delta G_{ij}^{(v)}$ and $\delta G_{ij}^{(w)}$ are the vertex and squark wave function corrections, respectively.

The vertex corrections $\delta G_{ij}^{(v)}$ are calculated from the graphs of Fig. 1b as

$$\delta G_{ij}^{(v)} = \frac{\alpha_s C_F}{4\pi} \left[\{ B_0(m_{t_i}^2, 0, m_{t_i}^2) + B_0(m_{b_j}^2, 0, m_{b_j}^2) - B_0(m_H^2, m_{t_i}^2, m_{b_j}^2) \right]$$

*Strictly speaking, our renormalization scheme is the $\overline{\text{DR}}'$ scheme [10] where the “ ϵ -scalar mass” is absorbed into $M_{\tilde{Q}, \tilde{U}, \tilde{D}}^2$.

$$\begin{aligned}
& -2(m_H^2 - m_{\tilde{t}_i}^2 - m_{\tilde{b}_j}^2)C_0(m_{\tilde{b}_j}^2, \lambda^2, m_{\tilde{t}_i}^2)\}G_{ij} \\
& -B_0(m_H^2, m_{\tilde{t}_k}^2, m_{\tilde{b}_l}^2)G_{kl}S_{ik}^{\tilde{t}}S_{lj}^{\tilde{b}} \\
& +2\{(\alpha_{LL})_{ij}(m_t y_2 + m_b y_1) + (\alpha_{RR})_{ij}(m_t y_1 + m_b y_2)\}B_0(m_H^2, m_b^2, m_t^2) \\
& +2\{(\alpha_{LL})_{ij}m_t y_2 + (\alpha_{LR})_{ij}m_{\tilde{g}}y_1 + (\alpha_{RL})_{ij}m_{\tilde{g}}y_2 + (\alpha_{RR})_{ij}m_t y_1\}B_0(m_{\tilde{t}_i}^2, m_{\tilde{g}}^2, m_t^2) \\
& +2\{(\alpha_{LL})_{ij}m_b y_1 + (\alpha_{LR})_{ij}m_{\tilde{g}}y_1 + (\alpha_{RL})_{ij}m_{\tilde{g}}y_2 + (\alpha_{RR})_{ij}m_b y_2\}B_0(m_{\tilde{b}_j}^2, m_{\tilde{g}}^2, m_b^2) \\
& +2\{(m_t^2 + m_b^2 - m_H^2)m_{\tilde{g}}((\alpha_{LR})_{ij}y_1 + (\alpha_{RL})_{ij}y_2) \\
& +(m_b^2 + m_{\tilde{g}}^2 - m_{\tilde{b}_j}^2)m_t((\alpha_{LL})_{ij}y_2 + (\alpha_{RR})_{ij}y_1) \\
& +(m_t^2 + m_{\tilde{g}}^2 - m_{\tilde{t}_i}^2)m_b((\alpha_{LL})_{ij}y_1 + (\alpha_{RR})_{ij}y_2) \\
& +2m_{\tilde{g}}m_t m_b((\alpha_{LR})_{ij}y_2 + (\alpha_{RL})_{ij}y_1)\}C_0(m_b^2, m_{\tilde{g}}^2, m_t^2)\Big], \tag{9}
\end{aligned}$$

where $C_F = 4/3$,

$$S^{\tilde{q}} = \begin{pmatrix} \cos 2\theta_{\tilde{q}} & -\sin 2\theta_{\tilde{q}} \\ -\sin 2\theta_{\tilde{q}} & -\cos 2\theta_{\tilde{q}} \end{pmatrix}, \tag{10}$$

$$\begin{aligned}
\alpha_{LL} &= \begin{pmatrix} \cos \theta_{\tilde{t}} \cos \theta_{\tilde{b}} & -\cos \theta_{\tilde{t}} \sin \theta_{\tilde{b}} \\ -\sin \theta_{\tilde{t}} \cos \theta_{\tilde{b}} & \sin \theta_{\tilde{t}} \sin \theta_{\tilde{b}} \end{pmatrix}, \quad \alpha_{LR} = \begin{pmatrix} -\cos \theta_{\tilde{t}} \sin \theta_{\tilde{b}} & -\cos \theta_{\tilde{t}} \cos \theta_{\tilde{b}} \\ \sin \theta_{\tilde{t}} \sin \theta_{\tilde{b}} & \sin \theta_{\tilde{t}} \cos \theta_{\tilde{b}} \end{pmatrix}, \\
\alpha_{RL} &= \begin{pmatrix} -\sin \theta_{\tilde{t}} \cos \theta_{\tilde{b}} & \sin \theta_{\tilde{t}} \sin \theta_{\tilde{b}} \\ -\cos \theta_{\tilde{t}} \cos \theta_{\tilde{b}} & \cos \theta_{\tilde{t}} \sin \theta_{\tilde{b}} \end{pmatrix}, \quad \alpha_{RR} = \begin{pmatrix} \sin \theta_{\tilde{t}} \sin \theta_{\tilde{b}} & \sin \theta_{\tilde{t}} \cos \theta_{\tilde{b}} \\ \cos \theta_{\tilde{t}} \sin \theta_{\tilde{b}} & \cos \theta_{\tilde{t}} \cos \theta_{\tilde{b}} \end{pmatrix}, \tag{11}
\end{aligned}$$

$$y_1 = \frac{g}{\sqrt{2}m_W}m_b \tan \beta = h_b \sin \beta, \quad y_2 = \frac{g}{\sqrt{2}m_W}m_t \cot \beta = h_t \cos \beta, \tag{12}$$

and $m_{\tilde{g}}$ is the gluino mass. A gluon mass λ is introduced to regularize the infrared divergences. Here we define the functions A , B_0 , B_1 and C_0 as in [11] ($\Delta = 2/(4 - D) - \gamma_E + \log 4\pi$):

$$\begin{aligned}
A(m^2) &= \int \frac{d^D q}{i\pi^2} \frac{1}{q^2 - m^2} = m^2(\Delta + \log(Q^2/m^2) + 1), \tag{13} \\
B_0(k^2, m_1^2, m_2^2) &= \int \frac{d^D q}{i\pi^2} \frac{1}{(q^2 - m_1^2)((q+k)^2 - m_2^2)}
\end{aligned}$$

$$= \Delta - \int_0^1 dz \log \frac{(1-z)m_1^2 + zm_2^2 - z(1-z)k^2 - i\delta}{Q^2}, \quad (14)$$

$$\begin{aligned} B_1(k^2, m_1^2, m_2^2) &= \frac{1}{k_\mu} \int \frac{d^D q}{i\pi^2} \frac{q_\mu}{(q^2 - m_1^2)((q+k)^2 - m_2^2)} \\ &= -\frac{\Delta}{2} + \int_0^1 dz z \log \frac{(1-z)m_1^2 + zm_2^2 - z(1-z)k^2 - i\delta}{Q^2}, \end{aligned} \quad (15)$$

$$\begin{aligned} C_0(m_1^2, m_2^2, m_3^2) &= \int \frac{d^D q}{i\pi^2} \frac{1}{(q^2 - m_1^2)((q+k_2)^2 - m_2^2)((q+p)^2 - m_3^2)} \\ &= -\int_0^1 dx \int_0^1 dy \int_0^1 dz \delta(1-x-y-z) \times \\ &\quad (xm_1^2 + ym_2^2 + zm_3^2 - xym_{b_j}^2 - yzm_{t_i}^2 - xzm_H^2 - i\delta)^{-1}. \end{aligned} \quad (16)$$

Here p and k_2 are respectively the external momenta of H^+ and \tilde{b}_j , and Q is the $\overline{\text{DR}}$ renormalization scale. Note that Δ is omitted in the $\overline{\text{DR}}$ scheme.

The squark wave function corrections $\delta G_{ij}^{(w)}$ are expressed as

$$\delta G_{ij}^{(w)} = -\frac{1}{2} [\dot{\Pi}_{ii}^{\tilde{t}}(m_{t_i}^2) + \dot{\Pi}_{jj}^{\tilde{b}}(m_{b_j}^2)] G_{ij} - \frac{\Pi_{ii'}^{\tilde{t}}(m_{t_i}^2)}{m_{t_i}^2 - m_{t_{i'}}^2} G_{i'j} - \frac{\Pi_{jj'}^{\tilde{b}}(m_{b_j}^2)}{m_{b_j}^2 - m_{b_{j'}}^2} G_{ij'}, \quad (17)$$

where $i \neq i'$ and $j \neq j'$. $\Pi_{ij}^{\tilde{q}}(k^2)$ are the one-loop corrections to the two-point functions of $\tilde{q}_i \tilde{q}_j$, which are obtained from the graphs of Fig. 1c. $\dot{\Pi}(k^2)$ denotes the derivative with respect to k^2 . The last two terms in (17) represent the corrections due to the renormalization of the \tilde{q} -mixings. The explicit forms are

$$\begin{aligned} \dot{\Pi}_{ii}^{\tilde{q}}(m_{\tilde{q}_i}^2) &= \frac{\alpha_s C_F}{4\pi} \left[-3B_0(m_{\tilde{q}_i}^2, 0, m_{\tilde{q}_i}^2) - 2B_1(m_{\tilde{q}_i}^2, 0, m_{\tilde{q}_i}^2) - 4m_{\tilde{q}_i}^2 \dot{B}_0(m_{\tilde{q}_i}^2, \lambda^2, m_{\tilde{q}_i}^2) \right. \\ &\quad - 2m_{\tilde{q}_i}^2 \dot{B}_1(m_{\tilde{q}_i}^2, 0, m_{\tilde{q}_i}^2) - 4m_{\tilde{g}}^2 \dot{B}_0(m_{\tilde{q}_i}^2, m_{\tilde{g}}^2, m_{\tilde{q}_i}^2) - 4B_1(m_{\tilde{q}_i}^2, m_{\tilde{g}}^2, m_{\tilde{q}_i}^2) \\ &\quad \left. - 4m_{\tilde{q}_i}^2 \dot{B}_1(m_{\tilde{q}_i}^2, m_{\tilde{g}}^2, m_{\tilde{q}_i}^2) + (-)^{i-1} 4 \sin 2\theta_{\tilde{q}} m_q m_{\tilde{g}} \dot{B}_0(m_{\tilde{q}_i}^2, m_{\tilde{g}}^2, m_q^2) \right], \end{aligned} \quad (18)$$

and

$$\Pi_{i'i}^{\tilde{q}}(m_{\tilde{q}_i}^2) = \frac{\alpha_s C_F}{4\pi} \left[\frac{1}{2} \sin 4\theta_{\tilde{q}} (A(m_{\tilde{q}_2}^2) - A(m_{\tilde{q}_1}^2)) + 4 \cos 2\theta_{\tilde{q}} m_q m_{\tilde{g}} B_0(m_{\tilde{q}_i}^2, m_{\tilde{g}}^2, m_q^2) \right]. \quad (19)$$

The one-loop corrected decay width in the $\overline{\text{DR}}$ scheme is then given by

$$\Gamma(H^+ \rightarrow \tilde{t}_i \bar{\tilde{b}}_j) = \frac{N_C \kappa_{\text{pole}}}{16\pi m_H^3} [|G_{ij}|^2 + 2G_{ij} \text{Re}(\delta G_{ij}^{(v)} + \delta G_{ij}^{(w)})]. \quad (20)$$

Here κ_{pole} refers to κ in (6) evaluated with pole squark masses. The width of (20) is infrared divergent.

In the numerical analysis we take the pole quark masses as inputs. The $\overline{\text{DR}}$ quark masses are obtained from the pole quark masses by using

$$\begin{aligned} m_q(Q)_{\overline{\text{DR}}} &= m_q(\text{pole}) - \frac{\alpha_s C_F}{4\pi} \left[2m_q(B_0(m_q^2, 0, m_q^2) - B_1(m_q^2, 0, m_q^2)) \right. \\ &\quad + \sin 2\theta_{\tilde{q}} m_{\tilde{g}} (B_0(m_q^2, m_{\tilde{g}}^2, m_{\tilde{q}_1}^2) - B_0(m_q^2, m_{\tilde{g}}^2, m_{\tilde{q}_2}^2)) \\ &\quad \left. + m_q(B_1(m_q^2, m_{\tilde{g}}^2, m_{\tilde{q}_1}^2) + B_1(m_q^2, m_{\tilde{g}}^2, m_{\tilde{q}_2}^2)) \right], \end{aligned} \quad (21)$$

which is derived from the graphs of Fig. 1d. Furthermore, in the phase space term κ_{pole} in (20) we have to take the pole squark masses given by

$$\begin{aligned} m_{\tilde{q}_i}^2(\text{pole}) &= m_{\tilde{q}_i}^2(Q)_{\overline{\text{DR}}} - \Pi_{ii}^{\tilde{q}}(m_{\tilde{q}_i}^2) \\ &= m_{\tilde{q}_i}^2(Q)_{\overline{\text{DR}}} + \frac{\alpha_s C_F}{4\pi} \left[-3A(0) + 4m_{\tilde{q}_i}^2 B_0(m_{\tilde{q}_i}^2, 0, m_{\tilde{q}_i}^2) + 2m_{\tilde{q}_i}^2 B_1(m_{\tilde{q}_i}^2, 0, m_{\tilde{q}_i}^2) \right. \\ &\quad - \cos^2 2\theta_{\tilde{q}} A(m_{\tilde{q}_i}^2) - \sin^2 2\theta_{\tilde{q}} A(m_{\tilde{q}_i'}^2) + 4A(m_q^2) \\ &\quad + 4m_{\tilde{g}}^2 B_0(m_{\tilde{q}_i}^2, m_{\tilde{g}}^2, m_q^2) + 4m_{\tilde{q}_i}^2 B_1(m_{\tilde{q}_i}^2, m_{\tilde{g}}^2, m_q^2) \\ &\quad \left. - (-)^{i-1} 4 \sin 2\theta_{\tilde{q}} m_q m_{\tilde{g}} B_0(m_{\tilde{q}_i}^2, m_{\tilde{g}}^2, m_q^2) \right]. \end{aligned} \quad (22)$$

4 Gluon emission

The infrared divergences in (20) are cancelled by including the $\mathcal{O}(\alpha_s)$ contribution from real gluon emission from \tilde{t} and $\bar{\tilde{b}}$ (Fig. 1e). The decay width of $H^+(p) \rightarrow$

$\tilde{t}_i(k_1) + \bar{\tilde{b}}_j(k_2) + g(k_3)$ is given in terms of the $\overline{\text{DR}}$ parameters as

$$\Gamma(H^+ \rightarrow \tilde{t}_i \bar{\tilde{b}}_j g) = \frac{\alpha_s C_F N_C |G_{ij}|^2}{4\pi^2 m_H} [(m_H^2 - m_{\tilde{t}_i}^2 - m_{\tilde{b}_j}^2) I_{12} - m_{\tilde{t}_i}^2 I_{11} - m_{\tilde{b}_j}^2 I_{22} - I_1 - I_2]. \quad (23)$$

The functions I_n , and I_{nm} are defined as [12]

$$I_{i_1 \dots i_n} = \frac{1}{\pi^2} \int \frac{d^3 k_1}{2E_1} \frac{d^3 k_2}{2E_2} \frac{d^3 k_3}{2E_3} \delta^4(p - k_1 - k_2 - k_3) \frac{1}{(2k_3 k_{i_1} + \lambda^2) \dots (2k_3 k_{i_n} + \lambda^2)}. \quad (24)$$

The explicit forms of $I_{i_1 \dots i_n}$ are given in [12]. In (23), $I_{11,22,12}$ are infrared divergent.

We have checked that the infrared divergences in (23) cancel those in (20). In the numerical analysis we define the corrected decay width as $\Gamma^{\text{corr}}(H^+ \rightarrow \tilde{t}_i \bar{\tilde{b}}_j) \equiv \Gamma(H^+ \rightarrow \tilde{t}_i \bar{\tilde{b}}_j) + \Gamma(H^+ \rightarrow \tilde{t}_i \bar{\tilde{b}}_j g)$.

5 Numerical results and conclusions

As in ref.[6], we choose $\{ m_H, m_{t,b}(\text{pole}), M, \mu, \tan \beta, M_{\tilde{Q}}, A \}$ as the basic input parameters of the MSSM, taking $M = (\alpha_2/\alpha_s)m_{\tilde{g}} = (3/5 \tan^2 \theta_W)M'$, $M_{\tilde{Q}} \equiv M_{\tilde{Q}}(Q)_{\overline{\text{DR}}} = M_{\tilde{U}}(Q)_{\overline{\text{DR}}} = M_{\tilde{D}}(Q)_{\overline{\text{DR}}} = M_{\tilde{L}}$ and $A \equiv A_t(Q)_{\overline{\text{DR}}} = A_b(Q)_{\overline{\text{DR}}} = A_\tau$. Here M (M') is the SU(2) (U(1)) gaugino mass, $\alpha_2 = g^2/4\pi$, and $(M_{\tilde{L}}, A_\tau)$ are the mass matrix parameters of the slepton sector [6]. The parameters M , M' , $M_{\tilde{L}}$, and A_τ do not receive $\mathcal{O}(\alpha_s)$ QCD corrections. The theoretical and experimental constraints for the basic input parameters are described in ref.[6]. We take $m_Z = 91.2\text{GeV}$, $m_W = 80\text{GeV}$, $m_t(\text{pole}) = 180\text{GeV}$ [13], $m_b(\text{pole}) = 5\text{GeV}$, $\sin^2 \theta_W = 0.23$ and $\alpha_2 = \alpha_2(m_Z) = \alpha/\sin^2 \theta_W = (1/129)/0.23 = 0.0337$. For the running QCD coupling at the renormalization scale Q , $\alpha_s = \alpha_s(Q)$, we always take the one-loop expression $\alpha_s(Q) = 12\pi/\{(33 - 2n_f) \ln(Q^2/\Lambda_{n_f}^2)\}$, with $\alpha_s(m_Z) = 0.12$, and the number of quark

flavors $n_f = 5(6)$ for $m_b < Q \leq m_t$ (for $Q > m_t$).

We define the QCD corrections as the difference between the $\mathcal{O}(\alpha_s)$ corrected width $\Gamma_{ij}^{\text{corr}} \equiv \Gamma^{\text{corr}}(H^+ \rightarrow \tilde{t}_i \bar{\tilde{b}}_j)$ of eqs.(20) plus (23) and the tree-level width $\Gamma_{ij}^{\text{tree}} \equiv \Gamma^{(0)}(H^+ \rightarrow \tilde{t}_i \bar{\tilde{b}}_j)$ of eq.(6) where $(m_q(\text{pole}), M_{\tilde{Q}}, A)$ are substituted for $(m_q, M_{\tilde{Q}, \tilde{U}, \tilde{D}}, A_q)$. The QCD corrections depend on the renormalization scale Q . We choose the optimum value of Q (Q_{opt}) such that $\Delta(Q) \equiv \sum_{q=t,b} \sum_{i=1,2} (m_{\tilde{q}_i}(\text{tree}) - m_{\tilde{q}_i}(\text{pole}))^2$ is minimized, where $m_{\tilde{q}_i}(\text{tree})$ refers to the \tilde{q}_i mass defined by (1–4) calculated with $m_q(\text{pole})$, $M_{\tilde{Q}}$, and A .

In order not to vary too many parameters, in the following we fix $\mu = 300\text{GeV}$, and take the values of M and $\tan \beta$ such that $m_{\tilde{\chi}_1^0} \simeq 50\text{GeV}$ as in [6] where $\tilde{\chi}_1^0$ is the lightest neutralino. In Fig.2 we show the m_H dependence of the tree-level and corrected widths $\Gamma^{\text{tree}}(\tilde{t}\bar{\tilde{b}}) \equiv \sum_{i,j=1,2} \Gamma_{ij}^{\text{tree}}$ and $\Gamma^{\text{corr}}(\tilde{t}\bar{\tilde{b}}) \equiv \sum_{i,j=1,2} \Gamma_{ij}^{\text{corr}}$, and the tree-level branching ratio $B^{\text{tree}}(\tilde{t}\bar{\tilde{b}}) \equiv \sum_{i,j=1,2} B^{\text{tree}}(H^+ \rightarrow \tilde{t}_i \bar{\tilde{b}}_j)$ [6] for (a) $M_{\tilde{Q}} = 250\text{GeV}$, $A = 650\text{GeV}$, $\tan \beta = 2$, $M = 120\text{GeV}$, and (b) $M_{\tilde{Q}} = 136\text{GeV}$, $A = 260\text{GeV}$, $\tan \beta = 12$, $M = 110\text{GeV}$. In these two cases we have (in GeV units): (a) $Q_{\text{opt}} = 216.5$, $m_{\tilde{g}} = 380$, $(m_{\tilde{t}_1}, m_{\tilde{t}_2}, m_{\tilde{b}_1}, m_{\tilde{b}_2})\{(\text{tree}), (Q_{\text{opt}})_{\overline{\text{DR}}}, (\text{pole})\} = \{(60, 429, 251, 254), (70, 420, 251, 254), (58, 428, 258, 262)\}$, $m_{\tilde{\chi}_1^+} = 94$, and (b) $Q_{\text{opt}} = 213.5$, $m_{\tilde{g}} = 349$, $(m_{\tilde{t}_1}, m_{\tilde{t}_2}, m_{\tilde{b}_1}, m_{\tilde{b}_2})\{(\text{tree}), (Q_{\text{opt}})_{\overline{\text{DR}}}, (\text{pole})\} = \{(81, 302, 62, 193), (74, 292, 120, 164), (66, 302, 126, 171)\}$, $m_{\tilde{\chi}_1^+} = 98$. Here $\tilde{\chi}_1^+$ is the lighter chargino. In both cases we see that the $\tilde{t}\bar{\tilde{b}}$ mode dominates the H^+ decay in a wide m_{H^+} range at the tree level, and that the QCD corrections to the $\tilde{t}\bar{\tilde{b}}$ mode are significant, but that as a whole they do not invalidate the $\tilde{t}\bar{\tilde{b}}$ mode dominance.

In Table 1 we show the values of the $B^{\text{tree}}(\tilde{t}\tilde{b})$, the QCD corrections $C \equiv (\Gamma^{\text{corr}}(\tilde{t}\tilde{b}) - \Gamma^{\text{tree}}(\tilde{t}\tilde{b}))/\Gamma^{\text{tree}}(\tilde{t}\tilde{b})$, and $C_{ij} \equiv (\Gamma_{ij}^{\text{corr}} - \Gamma_{ij}^{\text{tree}})/\Gamma_{ij}^{\text{tree}}$ for typical values of $M_{\tilde{Q}}$ and A , for (a) $m_{H^+} = 400\text{GeV}$, $\tan\beta = 2$, $M = 120\text{GeV}$, and (b) $m_{H^+} = 400\text{GeV}$, $\tan\beta = 12$, $M = 110\text{GeV}$. We see again that the $\tilde{t}\tilde{b}$ mode dominates in a wide region also when the QCD corrections are included. The QCD corrections can be very large at some points of $(M_{\tilde{Q}}, A)$; e.g. $C = -0.692$ at $(175\text{GeV}, 0\text{GeV})$ and $C_{12} = 0.734$ at $(225\text{GeV}, -350\text{GeV})$ in Table 1b. This occurs when $m_H \sim m_{\tilde{t}_i} + m_{\tilde{b}_j}$. This enhancement is just a kinematical effect due to the QCD corrections to $m_{\tilde{t}_i}$ and $m_{\tilde{b}_j}$.

In conclusion, we have calculated the $\mathcal{O}(\alpha_s)$ QCD corrections to the decay width of $H^+ \rightarrow \tilde{t}_i \tilde{b}_j$, including all quark mass terms and $\tilde{q}_L - \tilde{q}_R$ mixing. We find that the QCD corrections are significant but that they do not invalidate our previous conclusion at tree-level about the dominance of the $\tilde{t}\tilde{b}$ mode in a wide MSSM parameter region.

Acknowledgements

The work of Y.Y. was supported in part by the Fellowships of the Japan Society for the Promotion of Science and the Grant-in-Aid for Scientific Research from the Ministry of Education, Science and Culture of Japan, No. 06-1923 and 07-1923. The work of A.B., H.E., and W.M. was supported by the ‘‘Fonds zur F6rderung der wissenschaftlichen Forschung’’ of Austria, project no. P10843-PHY. The authors are grateful to Y. Kizukuri for the collaboration at the early stage of this work.

References

- [1] H. P. Nilles, Phys. Rep. 110 (1984) 1;
A. B. Lahanas and D. V. Nanopoulos, Phys. Rep. 145 (1987) 1;
R. Barbieri, Riv. Nuovo Cimento 11 (1988) 1.
- [2] H. E. Haber and G. L. Kane, Phys. Rep. 117 (1985) 75.
- [3] J. F. Gunion, H. E. Haber, G. L. Kane, and S. Dawson, The Higgs Hunter's Guide, Addison-Wesley (1990)
- [4] J. F. Gunion and H. E. Haber, Nucl. Phys. B272 (1986) 1; B402 (1993) 567 (E).
- [5] Z. Kunszt and F. Zwirner, Nucl. Phys. B385 (1992) 3.
- [6] A. Bartl, K. Hidaka, Y. Kizukuri, T. Kon and W. Majerotto, Phys. Lett. B315 (1993) 360.
- [7] C. S. Li and R. J. Oakes, Phys. Rev. D43 (1991) 855 ;
A. Méndez and A. Pomarol, Phys. Lett. B252 (1990) 461.
- [8] C. S. Li and J. M. Yang, Phys. Lett. B315 (1993) 367 ;
H. König, Mod. Phys. Lett. A10 (1995) 1113.
- [9] W. Siegel, Phys. Lett. 84B (1979) 193;
D. M. Capper, D. R. T. Jones and P. van Nieuwenhuizen, Nucl. Phys. B167 (1980) 479;
I. Antoniadis, C. Kounnas and K. Tamvakis, Phys. Lett. 119B (1982) 377.

- [10] I. Jack, D. R. T. Jones, S. P. Martin, M. T. Vaughn and Y. Yamada, Phys. Rev. D50 (1994) 5481.
- [11] G. 't Hooft and M. Veltman, Nucl. Phys. B153 (1979) 365;
G. Passarino and M. Veltman, Nucl. Phys. B160 (1979) 151.
- [12] A. Denner, Fortschr. Phys. 41 (1993) 307.
- [13] F. Abe et al. (CDF Collaboration), Phys. Rev. Lett. 74 (1995) 2626;
S. Abachi et al. (D0 Collaboration), Phys. Rev. Lett. 74 (1995) 2632;
K. Kleinknecht, talk at The XXXth Rencontre de Moriond “Electroweak interactions and unified theories”, Les Arcs, Savoie, 11-18 March, 1995.

Table 1

$B^{\text{tree}}(\tilde{t}\tilde{\bar{b}})$, C , and C_{ij} for typical values of $M_{\tilde{Q}}$ and A , for $(m_H(\text{GeV}), m_t(\text{pole})(\text{GeV}), M(\text{GeV}), \mu(\text{GeV}), \tan\beta) = (400, 180, 120, 300, 2)$ (a) and $(400, 180, 110, 300, 12)$ (b). The LEP bounds $m_{\tilde{q}, \tilde{l}, \tilde{\nu}} \gtrsim 45\text{GeV}$ and the requirement $m_{\tilde{t}_1, \tilde{b}_1, \tilde{l}} > m_{\tilde{\chi}_1^0} (\simeq 50\text{GeV})$ are satisfied. Q_{opt} denotes the optimum value of the renormalization scale Q as defined in the text. The * in the column of C_{ij} means that the $\tilde{t}_i\tilde{\bar{b}}_j$ channel is not open at the tree level and/or one-loop level. In Table 1b the columns of C_{21} and C_{22} are omitted, because the corresponding channels are not open, except $C_{21} = -0.141$ at $(M_{\tilde{Q}}, A) = (150\text{GeV}, 0\text{GeV})$.

(a)

$M_{\tilde{Q}}(\text{GeV})$	$A(\text{GeV})$	$B^{\text{tree}}(\tilde{t}\tilde{b})$	C	C_{11}	C_{12}	C_{21}	C_{22}	$Q_{\text{opt}}(\text{GeV})$
75	0	0.715	0.054	-0.251	0.143	0.025	0.664	224.0
75	200	0.793	0.158	-0.090	0.363	-0.211	0.319	225.0
75	300	0.818	0.161	-0.181	0.261	-0.229	0.363	240.5
100	0	0.690	0.090	-0.229	0.165	0.115	1.051	222.0
100	300	0.788	0.219	-0.166	0.295	-0.181	0.509	234.5
125	100	0.689	0.240	-0.170	0.332	0.127	0.891	217.5
125	350	0.702	0.175	-0.220	0.267	*	*	238.0
150	300	0.607	0.280	-0.124	0.402	*	*	221.0
150	400	0.719	0.159	-0.272	0.232	*	*	238.0
200	500	0.730	0.188	-0.375	0.215	*	*	226.5
250	650	0.752	0.209	-0.437	0.236	*	*	216.5

(b)

$M_{\tilde{Q}}(\text{GeV})$	$A(\text{GeV})$	$B^{\text{tree}}(\tilde{t}\tilde{b})$	C	C_{11}	C_{12}	$Q_{\text{opt}}(\text{GeV})$
150	-200	0.736	-0.152	-0.200	0.531	157.5
150	0	0.715	0.062	-0.383	*	159.0
150	250	0.740	-0.013	0.047	0.394	200.0
175	-250	0.651	0.120	-0.132	0.399	167.5
175	0	0.612	-0.692	-0.432	*	169.0
175	300	0.681	0.251	0.139	0.323	204.5
200	-300	0.606	0.169	-0.061	0.395	166.5
200	350	0.656	0.306	0.239	0.345	201.0
225	-350	0.512	0.352	0.012	0.734	161.5
225	400	0.588	0.501	0.355	0.587	193.5
250	500	0.616	0.383	0.579	0.319	193.5

Figure Captions

Fig.1 All diagrams relevant to the calculation of the $\mathcal{O}(\alpha_s)$ SUSY QCD corrections to the width of $H^+ \rightarrow \tilde{t}_i \tilde{b}_j$ in the MSSM.

Fig.2 The m_H dependence of $\Gamma^{\text{tree}}(\sum \tilde{t}_i \tilde{b}_j) \equiv \Gamma^{\text{tree}}(\tilde{t}\tilde{b})$ (dashed line), $\Gamma^{\text{corr}}(\sum \tilde{t}_i \tilde{b}_j) \equiv \Gamma^{\text{corr}}(\tilde{t}\tilde{b})$ (solid line), and $B^{\text{tree}}(\tilde{t}\tilde{b})$ (short-dashed line) for $(m_t(\text{pole})(\text{GeV}), M(\text{GeV}), \mu(\text{GeV}), \tan \beta, M_{\tilde{Q}}(\text{GeV}), A(\text{GeV})) = (180, 120, 300, 2, 250, 650)$ (a) and $(180, 110, 300, 12, 136, 260)$ (b). $\Gamma^{\text{tree}}(\tilde{t}_i \tilde{b}_j) \equiv \Gamma_{ij}^{\text{tree}}$ (dashed lines) and $\Gamma^{\text{corr}}(\tilde{t}_i \tilde{b}_j) \equiv \Gamma_{ij}^{\text{corr}}$ (solid lines) are separately shown for $(i, j) = (1, 1)$ and $(1, 2)$.

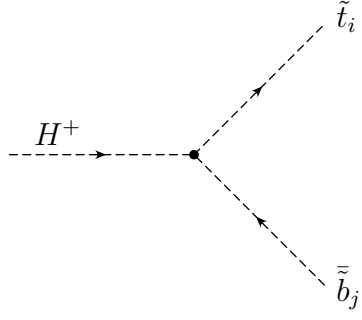


Fig. 1a

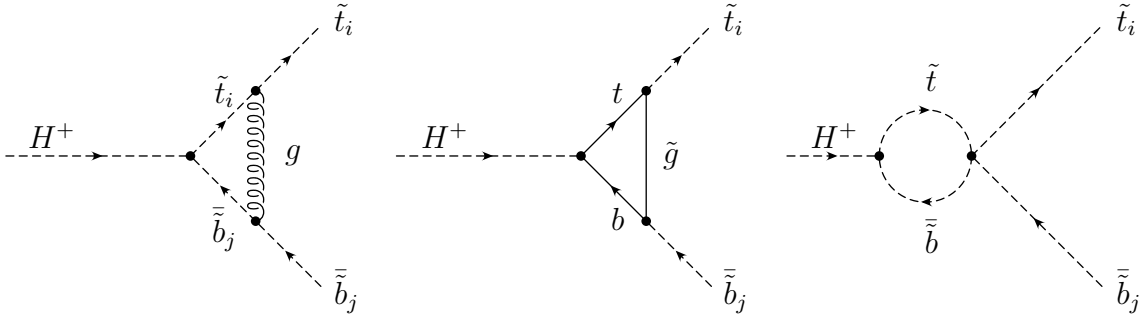


Fig. 1b

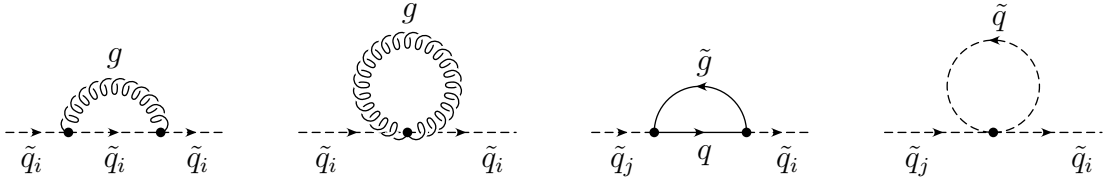


Fig. 1c

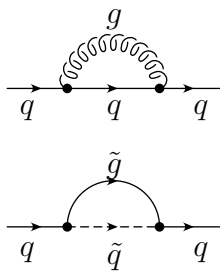


Fig. 1d

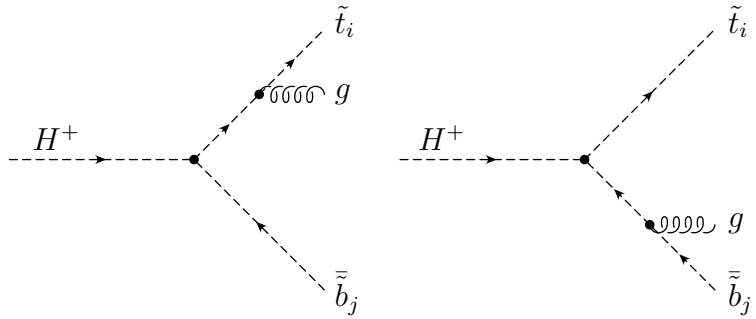


Fig. 1e

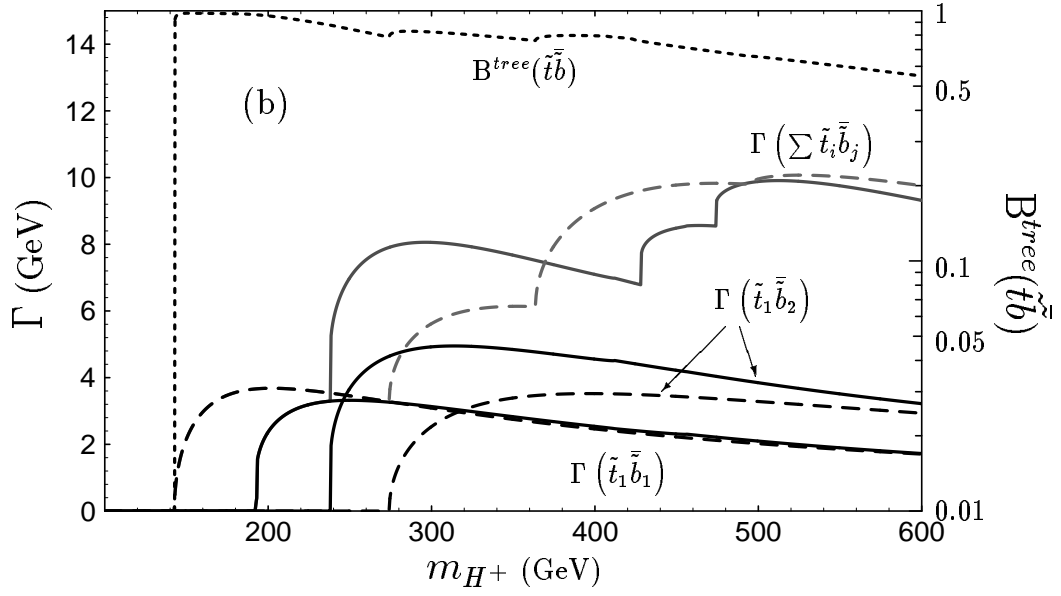
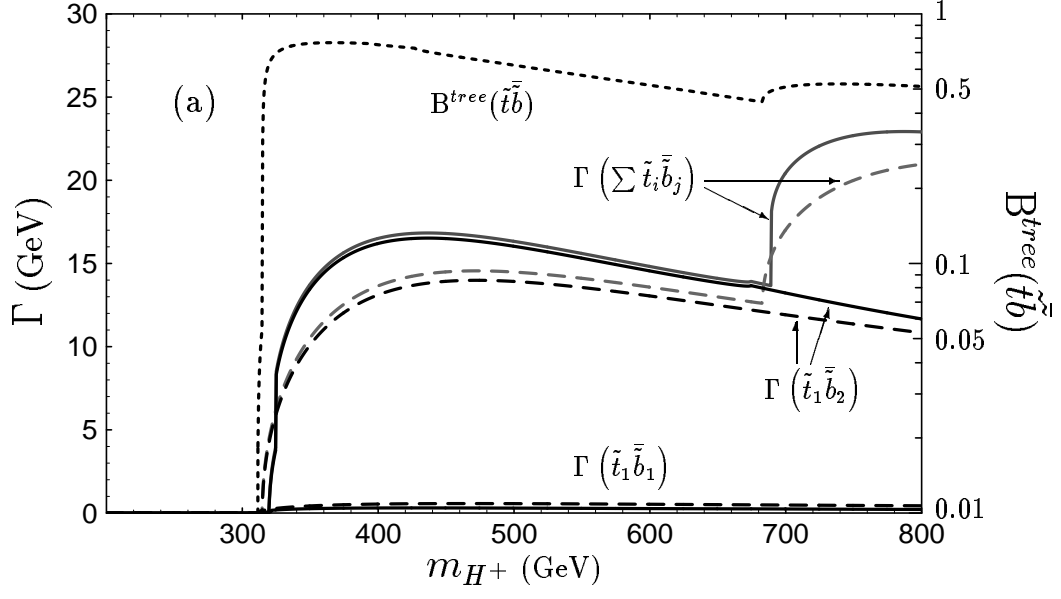


Fig. 2